ICMIEE 18-201

Finned-tube Heat Exchanger with Circular, Elliptical & Rectangular Tubes with Water-vapor as Working Fluid

Md. Hasibul Hasan[*], *Dipayan Mondal*
Department of Mechanical Engineering, Khulna University of Engineering & Technology, Khulna 9203, Bangladesh

ABSTRACT
3D numerical study has been conducted on the finned-tube heat exchanger with multiple rows of tubes using ANSYS. The objective of this study is to numerically investigate finned tube heat exchanger for multiple rows of tube with several types of tubes such as circular, elliptical and rectangular tubes with water-vapor. Heat transfer performance analysis has been performed for three and six rows of tube. Heat transfer characteristics were studied with various inlet air velocities. The results show that in the case of water-vapor, modified heat exchanger (HX) 1 & 2 have 3.48% decrease in heat transfer from conventional circular tube heat exchanger. Also modified HX 1 & 2 have 2.11% decrease in heat transfer from conventional elliptical tube heat exchanger. On the contrary, at high inlet velocity, modified HX 2 have 10.45% higher from grouped elliptical tube heat exchanger, for modified HX 6 gives 5.80% higher heat transfer from grouped elliptical tube heat exchanger when N=3. Again in case of water vapor when N=3 modified HX 2 gives 2.38% higher heat transfer than baseline HX 2. When N=6, for water-vapor, all modified heat exchanger have a lower heat transfer than the conventional heat exchanger. For water-vapor, when N=3, all modified heat exchanger has a lower pressure drop than the conventional elliptical heat exchanger.

Key Words: Finned-tube heat exchanger, Darcy friction factor, Nusselt Number, Heat transfer, Pressure Drop

1.0 Introduction

Fin Tube Heat Exchanger (FTHX) are most used for forced air heating and cooling system. Usually, liquid passing through the tube and water-vapor flows over fin and tube. Tubes have been taken as a staggered arrangement in this work. Circular cross-section tubes are widely used in FTHX. Elliptical tubes have been using in recent years. For having a better aerodynamic shape of an elliptical tube, there has some advantage in compactness, high heat transfer coefficient, and lower pressure drop. In this present analysis, for the first time, the rectangular tube has considered for numerical investigation. Many geometric parameters are related with FTHX like fin pitch, tube pitch, tube size & fin thickness. It is difficult to find out the best performance considering all parameters. Hence, early experimental studies conducted by Rich et al. [1] who investigated a total of fourteen tubes, in which the tube size was 13.34 mm. The corresponding longitudinal and transverse tube pitches were 27.5 and 31.75 mm, respectively. He examined the effect of fin spacing and the number of tube row and concluded that the heat transfer coefficient was essentially independent of the fin spacing's and the pressure drop per row are independent of the number of tube rows [2]. 2D heat transfer analysis was performed by with one & two rows tube where only circular & elliptical tubes have been examined with experimentally determined heat transfer coefficient from heat & mass transfer analogy. Temperature distribution on the fin & air stream were determined Rocha et al. [3].

2.1 Problem statement

Plate-fin with staggered tube arrangement has taken to study with water-vapor heat transfer and pressure drop characteristics. To closely represent the real-time heat exchanger, multiple tube rows (number of tube rows, N = 3, 6) are considered. The effect of a number of tubes has also been studied. When the tube number exceeds six, the corresponding increase in heat transfer is negligible [4], therefore present work concerns up to six rows of tube.

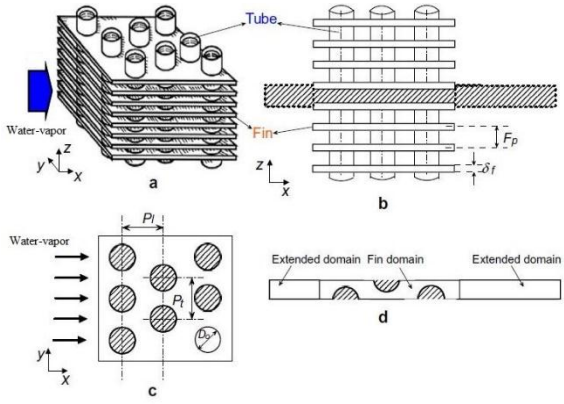

Fig 1: Schematic configuration of a heat exchanger (a) The overall core: air flows across the finned bundle. (b) Cross-section in z–x plane surfaces (c) Cross-section in y–x plane (d) Cross-section of computational domain in y–x plane [4].

The circular and elliptical tubes are designed in such a way that perimeter of the tubes are same, which allows ease of manufacturing and ensures same heat transfer

* Corresponding author. Mob: +8801751321986
E-mail address: hasibulshovon@gmail.com

Area for the circular, elliptical and rectangular tube. The eccentricity of the elliptical tube is taken as which is closer to Rocha et al [3]. As the region of interest of the present work is focused on to identify the tube geometric effect, the fin surface is assumed to be a constant wall temperature. Geometric parameters are taken from Deepakkumar et al. [5] where fin length is a product of number of tubes and longitudinal pitch.

2.2 Geometric Details

In this present investigation, there is three type of tube, so total $3P_3$=6 combinations are possible as shown in Table 1. But for 6 rows of tube, those combinations are doubled in a staggered arrangement.

Designation	Schematic Representation	Category
N3B1		Baseline-1
N3B2		Baseline-2
N3M1		Modified-1
N3M2		Modified-2
N3M3		Modified-3
N3M4		Modified-4
N3M5		Modified-5
N3M6		Modified-6
N6B1		Baseline-1
N6B2		Baseline-2
N6M1		Modified-1
N6M2		Modified-2
N6M3		Modified-3
N6M4		Modified-4
N6M5		Modified-5
N6M6		Modified-6

Table 1: Combination of the tube in the various arrangement.

2.3 Grid Generation and Solution Methodology

The computational domain is discretized into a finite number of control volume. In fin region, inflation mesh control is done with four edges of circular and elliptical in both sides. First layer thickness inflation option is selected as shown in Fig 2. After that body sizing is done on fin region. In the upstream and downstream region, several edge sizing is done in various direction.

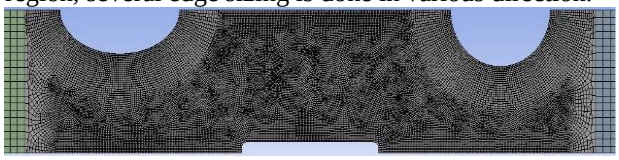

Fig 2: Schematic representation of the grid.

The finite volume based CFD code ANSYS Fluent 16.2 is used to calculate the flow and temp fields and by applying SIMPLEC algorithm. Fluid properties has been selected as water vapor from ANSYS fluent database. Under relaxation factor for pressure correction is taken as 1 for faster convergence. Boundary Condition has taken from the paper of Han et al [6]. Inlet has taken as velocity inlet and outlet as outflow boundary condition. Fin region portion has taken as wall with constant temp. Tube surface has also taken as constant wall temperature. To obtain improved accuracy of the solution, second-order spatial discretization of pressure is employed. As the grids are structured hexahedral and are aligned with flow direction, QUICK scheme is used for discretizing higher-order convective terms in the momentum equation. The residual is 10^{-6} for continuity and momentum, 10^{-8} for energy equation.

2.4 Definition Parameter

The definitions of non-dimensional parameters such as Reynolds number (Re), Nusselt number (Nu) and Darcy friction factor (f) are defined as follows [7],

$$LMTD = \frac{(T_w - T_{in}) - (T_w - T_{out})}{ln\frac{(T_w - T_{in})}{(T_w - T_{out})}} \quad (1)$$

Heat Transfer rate

$$Q = mC_p(T_{out} - T_{in}) \quad (2)$$

$$h_m = \frac{Q}{LMTD \times A_s} \quad (3)$$

$$f = \frac{\Delta P}{0.5\,\rho U_{in}^{\,2}} \frac{H}{L} \quad (4)$$

3.1 Result Validation

The present results are validated with the experimental work of Wang and Chi [8] and a close agreement has been observed as shown in Fig 3.

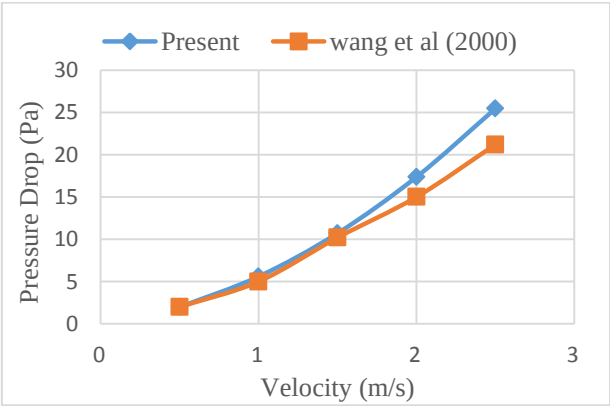

Fig 3: Validation results for N=2

3.2 Mesh dependency

For checking mesh dependency baseline N3B1 has taken for consideration. Grid 1 = 264935 nodes, Grid 2 = 361911 nodes, Grid 3 = 498982 nodes. Mesh dependency has been checked for heat transfer coefficient at different inlet velocity. From Fig 4, it is observed that at grid 1 and grid 3 gives almost the same heat transfer coefficient. For further calculation, grid 1 has taken as the best option considering time for a solution to converge.

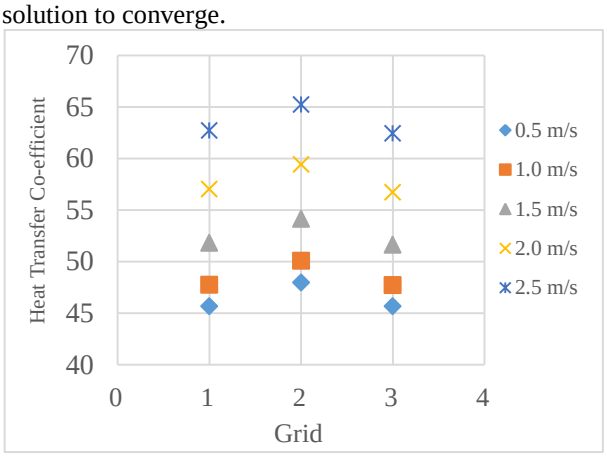

Fig 4: Grid independence results (N=3)

3.3.1 Heat Transfer rate for water-vapor

The result has been presented on Normalized Nu number and friction factor. The results are normalized (Xi/Xo), where i stands for modified cases and o stands for baseline cases. Water vapor is also taken in steads of air with all those combinations. Due to having different properties of water vapor, there is the difference in heat transfer and Nusselt number rather than air. The circular tube has a higher heat transfer rate than elliptical and rectangular tubes. Heat transfer for elliptical tube almost half than circular tubes [9].

From Fig 5, Heat transfer for N3M1 is lower at all inlet velocity than N3B2 for this reason slope of the curve is downward. But reverse action is shown for N3M2 when compared with N3B2. From Fig 6, for water-vapor N3M3 and N3M4 both have low heat transfer rate from low inlet velocity to high inlet velocity when compared with N3B1. Similar things happen for N3M3 and N3M4 when compared with N3B2. From Fig 7, these combinations are better than previous two named as N3M3 and N3M4. For water-vapor N3M5 and N3M6, both have low heat transfer rate from low inlet velocity to high inlet velocity when compared with N3B1. Similar things happen for N3M5 and N3M6 when compared with N3B2.

From Fig 8, this case is for six rows of tube. N6M1 and N6M2 are compared with N6B1, at that time heat transfer are so much lower in high inlet velocity. But N6M1 and N6M2 have also compared with N6B2 which is better than N6B1. From Fig 10, this is also similar to the previous two combination Heat transfer rate for N6M5 and N6M6 when compared with N6B2 decreases up to velocity 2 m/s is similar when velocity 2.5m/s N6M6 decreases more than N6M5.

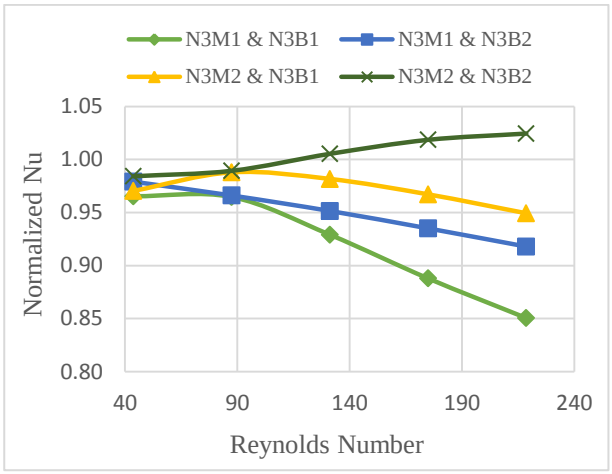

Fig 5: Normalized Nu VS Re number for N3M1 & N3M2 w.r.t N3B1 & N3B2

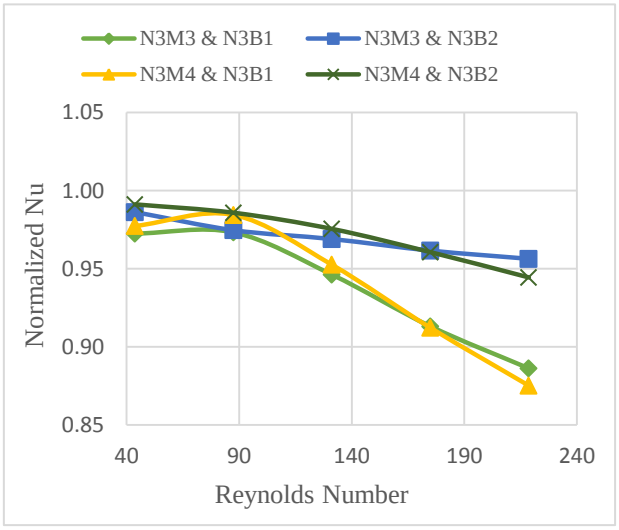

Fig 6: Normalized Nu VS Re number for N3M3 & N3M4 w.r.t N3B1 & N3B2

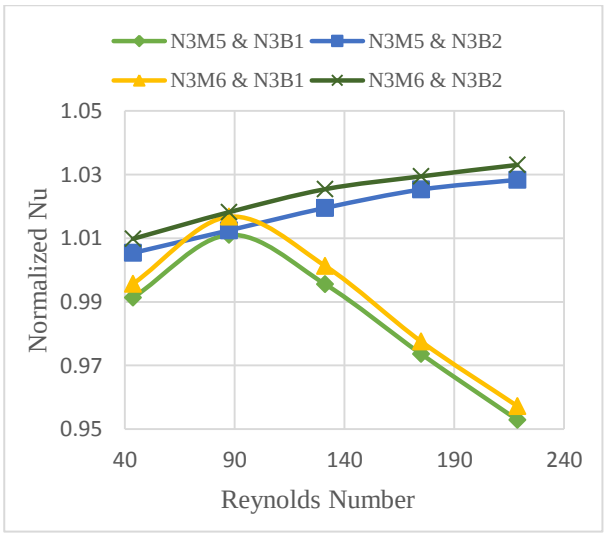

Fig 7: Normalized Nu VS Re number for N3M5 & N3M6 w.r.t N3B1 & N3B2

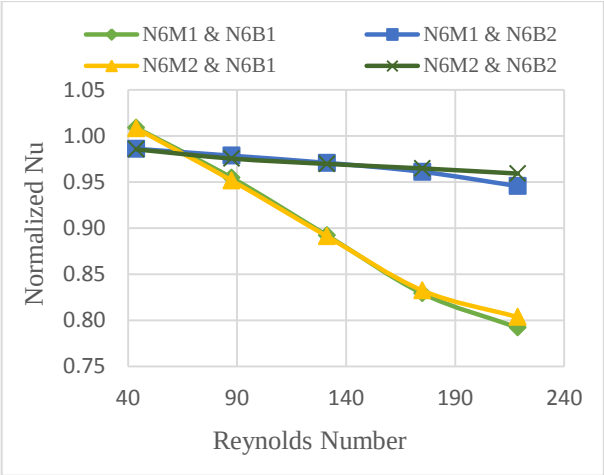

Fig 8: Normalized Nu VS Re number for N6M1 & N6M2 w.r.t N6B1 & N6B2

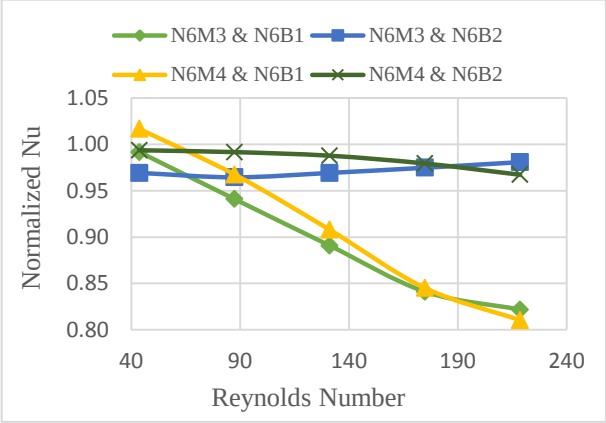

Fig 9: Normalized Nu VS Re number for N6M3 & N6M4 w.r.t N6B1 & N6B2

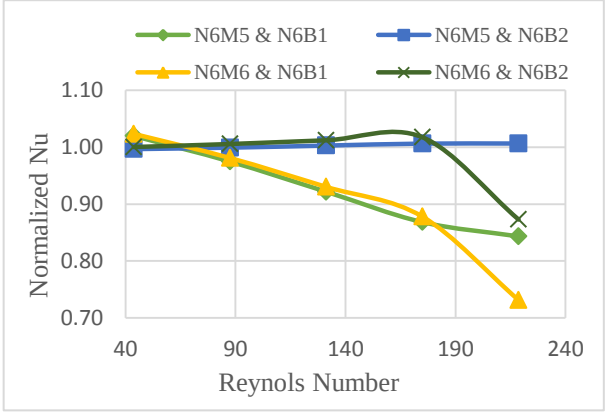

Fig 10: Normalized Nu VS Re number for N6M5 & N6M6 w.r.t N6B1 & N6B2

3.3.2 Friction factor for water-vapor

From Fig 11, N3M1 is better when compared with N3B2 because it has a lower friction coefficient. It is shown that friction for N3M2 increases having high friction factor. In contrast, the friction factor for N3M1 decreases when compared with N3B2. N3M1 combination is better when compare with N3B1. From Fig 12, it is observed that at low inlet velocity for N3M3 and N3M4, as velocity increases pressure drop reduces when both are compared with N3B1. From Fig 13, it is shown that for N3M5 and N3M6 pressure drop reduces as velocity increases when compared with N3B1.

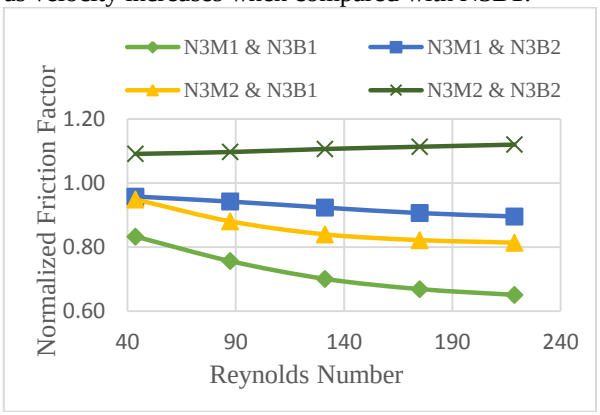

Fig 11: Normalized friction factor VS Re number for N3M1 & N3M2 w.r.t N3B1 & N3B2

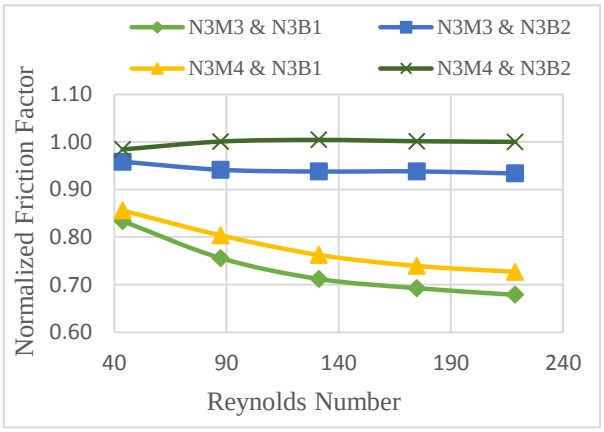

Fig 12: Normalized friction factor VS Re number for N3M3 & N3M4 w.r.t N3B1 & N3B2

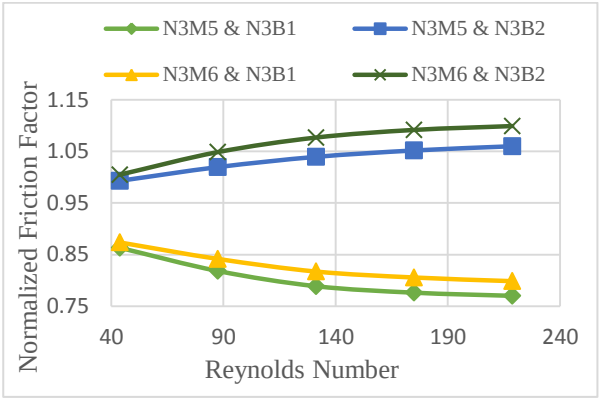

Fig 13: Normalized friction factor VS Re number for N3M5 & N3M6 w.r.t N3B1 & N3B2

From Fig 14, it is shown that N6M2 is one of the best combinations because it has much lower friction factor. For N6M2 pressure drop is higher when compared with N6B2 but friction factor decreases as velocity increases. N6M1 also have lower pressure drop when compared with N6B1 than N6B2. From Fig 15, it is inspected that, with increasing velocity, friction factor for N6M3 & N6B1 reduces while friction factor for N6M3 & N6B2 increases. N6M3 & N6B1 and N64 & N6B1 are similar their value of friction factor increases from 0.98 and 0.94 respectively. From Fig 16, it is shown for six rows

of tube that for N6M5 and N6M6 pressure drop reduces as velocity increases when compared with N6B1. Reverse action occurs when compared with N6B2.

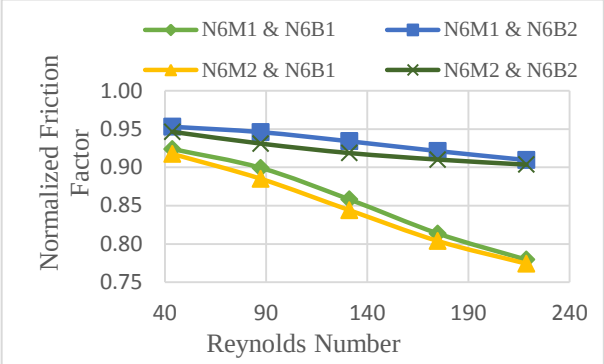

Fig 14: Normalized friction factor VS Re number for N6M1 & N6M2 w.r.t N6B1 & N6B2

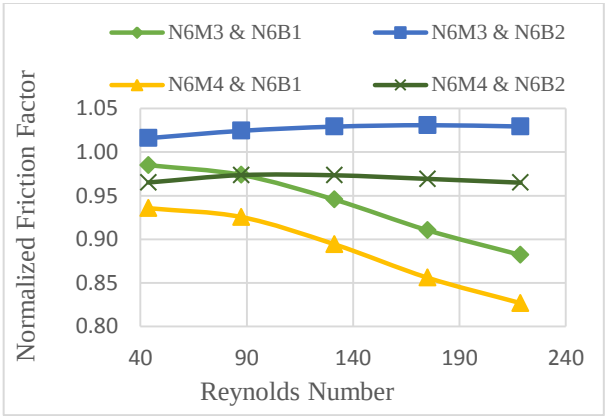

Fig 15: Normalized friction factor VS Re number for N6M3 & N6M4 w.r.t N6B1 & N6B2

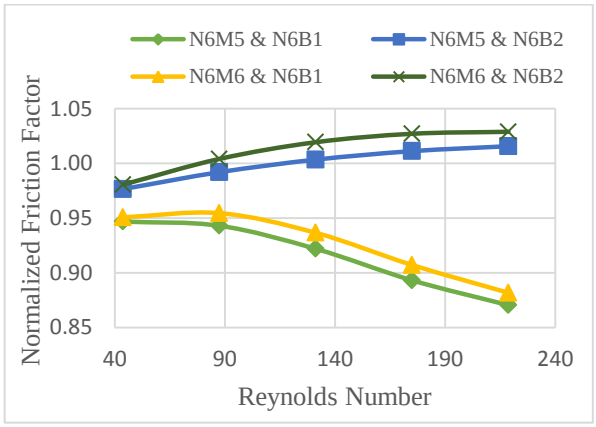

Fig 16: Normalized friction factor VS Re number for N6M5 & N6M6 w.r.t N6B1 & N6B2

3.4.1 Temperature contour of water-vapor

The temperature distribution is shown for water-vapor for three rows of tube. There is little difference in the outlet temp of water-vapor than air.

a) Temperature contour color legend

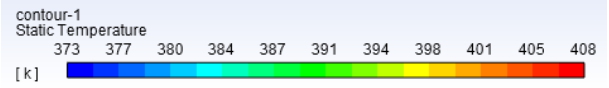

b) Geometry N3B1 0.5 m/s

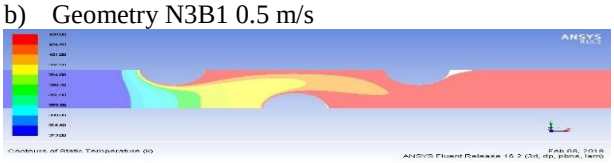

c) Geometry N3B1 2.5 m/s

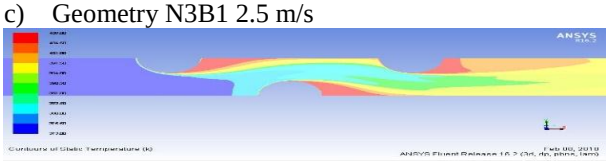

d) Geometry of N3M3 at 0.5 m/s

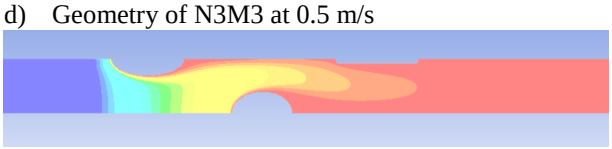

e) Geometry of N3M3 at 2.5 m/s

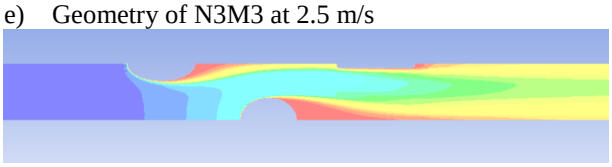

Fig 17: Temperature contour of water-vapor **a)** Temperature contour color legend **b)** N3B1 at 0.5 m/s **c)** N3B1 at 0.5m/s **d)** N3M3 at 0.5 m/s **e)** N3M3 at 2.5 m/s

3.4.2 Pressure contour of water-vapor

Static pressure distribution is shown for water-vapor are presented for one baseline case another for the modified case.

a) Geometry N3B1 for 0.5 m/s

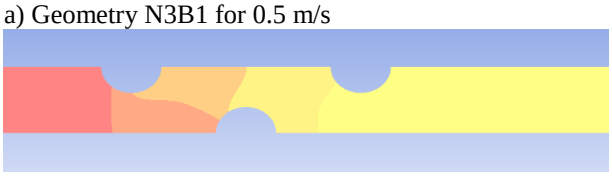

b) Geometry N3B1 for 2.5 m/s

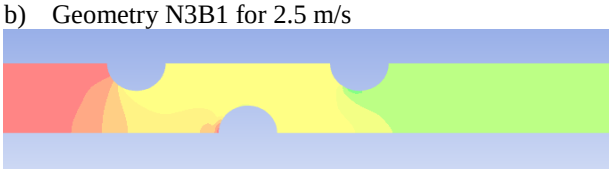

c) Geometry of N3M3 at 0.5 m/s

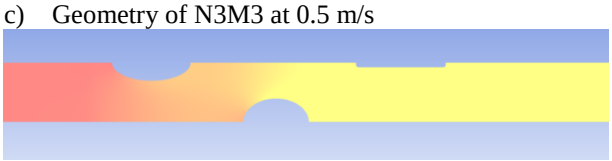

d) Geometry of N3M3 at 2.5 m/s

Fig 18: Pressure contour for water-vapor **a)** N6B1 at 0.5 m/s **b)** N6B1 at 2.5 m/s **c)** N3M3 at 0.5 m/s **d)** N3M3 at 2.5 m/s

3.5 Discussion

In this present simulation, water-vapor has been used as a fluid which passes over the tube. Several types of tubes have been considered for an investigation like circular, rectangular and elliptical. Several types of geometries named as a baseline and modified have been simulated. A number of tubes of rows have taken as three and six. There are some geometries which give lower friction factor than the conventional heat exchanger. On the other hand, gives a higher heat transfer coefficient than the conventional heat exchanger. Modified case 1 & 2 have 3.48% decrease in heat transfer from conventional circular tube heat exchanger. Also modified case 1 & 2 have 2.11% decrease in heat transfer from conventional elliptical tube heat exchanger. On the contrary, at high inlet velocity, modified case 2 have 10.45% higher from grouped elliptical tube heat exchanger, for modified case 6 gives 5.80% higher heat transfer from grouped elliptical tube heat exchanger when N=3. Again in case of water vapor when N=3 modified case 2 gives 2.38% higher heat transfer than baseline case 2 When N=6, for water-vapor, all modified heat exchanger have lower heat transfer than conventional heat exchanger 1.41 % of error occurred with the actual co-relation result. This has been due to flow separation point of the fluid over the tube surface. As long as flow adhered to the tube surface, fluid was heated up. Vortex generator could have been used to delay flow separation.

4.0 Conclusion

Water-vapor heat transfer characteristics for a different arrangement of circular, elliptical and rectangular tubes, has been numerically investigated in the laminar flow region for multiple rows. The heat exchanger with geometry N3M1 and N3M2 has been performed quite better than both circular and elliptical tubes. Similar performance has been observed for geometry N6M5 and N6M6 when compared with a conventional heat exchanger. The frictional resistance for water-vapor N3M1 N3M3 and N3M4 all have performed better than grouped circular and elliptical tubes. N6M1 and N6M2 have acted better than grouped circular tubes heat exchanger. N6M4 also performed better than grouped elliptical tubes.

Nomenclature

Symbol	Description
Cp	Specific heat capacity in J/Kg K
D	Diameter of the circular tube in m
f	Darcy Friction factor
H	Fin Height in m
h	heat transfer coefficient in W/m^{2}k
j	Nusselt number
k	Thermal conductivity in W/m-k
L	Length of fin in m
m	Mass flow rate of air in Kg/s
N	number of tube rows
Nu	Nusselt number
Pr	Prandtl number
Q	Heat transfer rate in W
Re	Reynolds number
T	Temperature in K
U	x-component velocity at inlet in m/s
Δp	Pressure drop in N/m^2
ΔT_{lm}	Logarithmic mean temperature difference
B	Conventional Heat Exchanger
M	Modified Heat Exchanger

References

[1] Rich DG. The effect of fin spacing on the heat transfer and friction performance of multi-row, smooth plate fin-and-tube heat exchangers. ASHRAE Trans 1973; 79(1):137–45.

[2] Lu CW, Huang JM, Nien WC, Wang CC, "A numerical investigation of the geometric effects on the performance of plate finned-tube heat exchanger", Energy Conversion Manage 2011; 52:1638-43.

[3] Rocha LAO, Saboya FEM, Vargas JVC, "A comparative study of elliptical and circular sections in one- and two-row tubes and plate fin heat exchangers" International Journal Heat Fluid Flow 1997, 18:247-252.

[4] Xie G, Wang Q, Sunden B, "Parametric study and multiple correlations on air-side heat transfer and friction characteristics of fin-and-tube heat exchangers with large number of large-diameter tube rows", Applied Thermal Engineering 2009; 29:1-16

[5] R. Deepakkumar, S. Jayavel, "Airside performance of finned-tube heat exchanger with combination of circular and elliptical tubes", Applied Thermal Engineering (2017),

[6] Hui Han, Ya-Ling He, Yin-Shi Li, Yu Wang, "A numerical study on compact enhanced fin-and-tube heat exchangers with oval and circular tube configurations", International Journal of Heat and Mass Transfer 65 (2013) 686–695

[7] F. Kreith, Raj M. Manglik, Mark S. Bohn, "Principles of Heat Transfer", Seventh Edition, Cengage Learning Inc. 2011

[8] Wang CC, Chi KY, Chang CJ, "Heat transfer and friction characteristics of plain finned- tube heat exchangers, part II: Correlation", International Journal Heat Mass Transfer 2000; 43:2693-700.

[9] Jang JY, Yang JY, "Experimental and 3-D Numerical Analysis of the Thermal-Hydraulic Characteristics of Elliptic Finned-Tube Heat Exchangers", Heat Transfer Engineering 1998, 19:55-67.